BIOCHEMISTRY
including biophysical chemistry & molecular biology

Article

pubs.acs.org/biochemistry

Effect of Charged Amino Acid Side Chain Length at Non-Hydrogen Bonded Strand Positions on β-Hairpin Stability

Li-Hung Kuo,[†] Jhe-Hao Li,[†] Hsiou-Ting Kuo,[†] Cheng-Yun Hung,[†] Hsin-Yun Tsai,[†] Wen-Chieh Chiu,[†] Cheng-Hsun Wu,[†] Wei-Ren Wang,[†] Po-An Yang,[†] Yun-Chiao Yao,[†] Tong Wai Wong,[†] Shing-Jong Huang,[‡] Shou-Ling Huang,[‡] and Richard P. Cheng*[,†]

[†]Department of Chemistry, National Taiwan University, Taipei 10617, Taiwan

[‡]Instrument Center at National Taiwan University, National Taiwan University, Taipei 10617, Taiwan

Supporting Information

ABSTRACT: β-Sheets have been implicated in various neurological disorders, and ∼20% of protein residues adopt a sheet conformation. Therefore, studies on the structural origin of sheet stability can provide fundamental knowledge with potential biomedical applications. Oppositely charged amino acids are frequently observed across one another in antiparallel β-sheets. Interestingly, the side chains of natural charged amino acids Asp, Glu, Arg, Lys have different numbers of hydrophobic methylenes linking the backbone to the hydrophilic charged functionalities. To explore the inherent effect of charged amino acid side chain length on antiparallel sheets, the stability of a designed hairpin motif containing charged amino acids with varying side chain lengths at non-hydrogen bonded positions was studied. Peptides with the guest position on the N-terminal strand and the C-terminal strand were investigated by NMR methods. The charged amino acids (Xaa) included negatively charged residues with a carboxylate group (Asp, Glu, Aad in increasing length), positively charged residues with an ammonium group (Dap, Dab, Orn, Lys in increasing length), and positively charged residues with a guanidinium group (Agp, Agb, Arg, Agh in increasing length). The fraction folded and folding free energy for each peptide were derived from the chemical shift deviation data. The stability of the peptides with the charged residues at the N-terminal guest position followed the trends: Asp > Glu > Aad, Dap < Dab < Orn ∼ Lys, and Agb < Arg < Agh < Agp. The stability of the peptides with the charged residues at the C-terminal guest position followed the trends: Asp < Glu < Aad, Dap ∼ Dab < Orn ∼ Lys, and Agb < Arg ∼ Agp < Agh. These trends were rationalized by thermodynamic sheet propensity and cross-strand interactions.

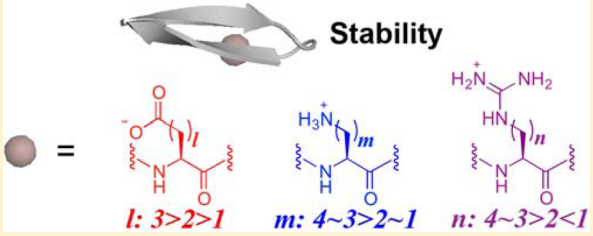

Proteins are a diverse group of biomacromolecules responsible for a wide array of biochemical functions.[1,2] A well-defined three-dimensional protein conformation can provide a structural platform to place crucial chemical functional groups in the appropriate orientations to support the biochemical function of the macromolecule. The hierarchical nature of protein folding and structure suggests that the fundamental building blocks of protein three-dimensional structures are the secondary structures such as α-helices and β-sheets.[3,4] According to surveys on protein structures, more than 30% of protein residues adopt an α-helix conformation,[5−10] whereas around 20% adopt an extended sheet conformation.[5,11] β-Sheet structures have been implicated in various human neurological disorders such as Crutzfeldt-Jacob (prion disease),[12,13] Huntington,[14,15] Alzheimer's,[16,17] and Parkinson's diseases.[18,19] Therefore, studies on the sequence and structural origin of sheet stability and formation can provide fundamental knowledge on protein structure with potential biomedical applications.

Initial studies on the intrinsic thermodynamic sheet propensity of the canonical 20 amino acids have provided the foundation for more complicated investigations on sheet energetics.[20−23] The effect of introducing the amino acid of interest in a β-sheet moiety showed some general trends with varying details.[20−23] In general, β-branched amino acids are most suitable for forming stable sheet structures.[20−23] However, thermodynamic sheet propensity is context dependent and can be easily influenced by cross-strand interactions.[22,24] As such, cross-strand interactions have been measured in sheet-containing host systems including the protein G B1 domain,[24−26] zinc finger domain,[27] and short hairpin constructs.[28−35] Interestingly, surveys on cross-strand sequence patterns have shown that oppositely charged amino acids are frequently observed directly across one another in antiparallel sheet structures,[36] suggesting specific ion pairing interactions.

The cross-strand ion pairing interaction energetics have been determined in both proteins and model hairpin peptides.[24,30,37−39] For the protein G B1 domain, a cross-strand lateral Glu-Lys ion pairing interaction increased the stability by 1.0 kcal/mol based on thermal denaturation studies.[24] For short hairpin peptides, cross-strand lateral Glu-Lys ion pairing

Received: July 10, 2013
Revised: October 7, 2013
Published: October 24, 2013

   dx.doi.org/10.1021/bi400911p | *Biochemistry* 2013, 52, 7785−7797

interactions provided 0.1−0.3 kcal/mol stability based on NMR methods.[30,38,39] Furthermore, the cross-strand lateral Glu-Lys ion pairing interaction closer to the turn was stronger compared to the same interaction closer to the termini in a hairpin forming peptide,[39] most likely due to end fraying effects.[39] In addition, a cross-strand backbone to side chain ion pairing interaction provided 0.2−0.3 kcal/mol stability in a hairpin peptide based on NMR methods.[37]

Ion pairing interactions can occur between oppositely charged amino acids on neighboring strands. Interestingly, the side chains of encoded charged amino acids Asp, Glu, Arg, and Lys have different numbers of hydrophobic methylenes linking the backbone to the hydrophilic charged functionality (Figure 1). The effect of the number of methylenes on

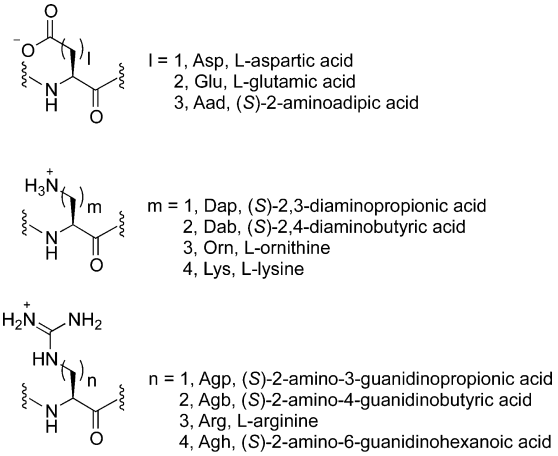

Figure 1. Chemical structures of the analogues of aspartate, arginine, and lysine with varying side chain length.

thermodynamic helix propensity has been thoroughly studied.[9,40,41] For the negatively charged amino acids, increasing the side chain length of Asp to Glu increases the helix propensity.[40,42,43] For Lys analogues with an ammonium group, the helix propensity also increases with side chain length.[41] In contrast, for Arg analogues with a guanidinium group, Arg exhibits the highest helix propensity;[9] either lengthening or shortening the Arg side chain length decreases the helix propensity.[9] Analogous studies on sheet propensity have been more limited.[20−23] Asp and Glu showed similar sheet propensities in studies on a zinc finger domain.[20] However, the sheet propensity in the protein G B1 domain increased upon increasing the side chain length from Asp to Glu.[21−23] The sheet propensity of Lys apparently decreased upon shortening the side chain length in a β-hairpin motif;[44] however, the effect of lateral and diagonal cross-strand interactions seemed present and could not be completely ruled out. Herein, we present a systematic study on the effect of charged amino acid side chain length at non-hydrogen bonded positions on the stability of a designed hairpin motif based on NMR methods.

MATERIALS AND METHODS

Peptide Synthesis. Peptides were synthesized by solid phase peptide synthesis using Fmoc-based chemistry.[45,46] Peptides containing (*S*)-2-amino-3-guanidinopropanoic acid (Agp) and (*S*)-2-amino-6-guanidinohexanoic acid (Agh) were synthesized by standard coupling protocols using the protected residues Fmoc-Agp(Boc)$_2$−OH and Fmoc-Agh(Boc)$_2$−OH,[9] respectively. Peptides containing (*S*)-2-amino-4-guanidinobutanoic acid (Agb) were synthesized by solid phase guanidinylation using established protocols.[9,47] The disulfide bond of the folded reference peptides (HPTFXaaAla and HPTFAlaXaa) were formed via charcoal mediated air oxidation.[48] All peptides were purified by reverse-phase high-performance liquid chromatography to greater than 95% purity. The identity of the peptides was confirmed by matrix-assisted laser desorption ionization-time-of-flight mass spectrometry (MALDI-TOF MS). More detailed procedures and peptide characterization data are provided in the Supporting Information.

Nuclear Magnetic Resonance Spectroscopy. NMR samples were prepared by dissolving the lyophilized purified peptides with purity above 95% into H_2O/D_2O (9:1 ratio by volume) in the presence of 50 mM sodium deuterioacetate buffer (uncorrected pH 5.5) to give peptide concentrations of 1−10 mM. 2-Dimethyl-2-silapentane-5-sulfonate (DSS) was added to the samples as an internal reference. All NMR experiments were performed on a Brüker AV III 800 MHz spectrometer. Phase-sensitive double-quantum filtered-correlated spectroscopy (DQF-COSY),[49] total correlation spectroscopy (TOCSY),[50] nuclear Overhauser effect spectroscopy (NOESY),[51] and rotating-frame nuclear Overhauser effect spectroscopy (ROESY)[52] experiments were performed by collecting 2048 points in $f2$ with 4−8 scans and 256−512 points in $f1$. Solvent suppression was achieved by the WATERGATE solvent suppression sequence.[53,54] TOCSY and ROESY experiments employed a spin locking field of 10 kHz. Mixing times of 60, 120, and 200 ms were used for the TOCSY, NOESY, and ROESY experiments, respectively.

Chemical Shift Deviation. Sequence specific assignments for all peptides were completed by using the 2D-NMR spectra (DQF-COSY,[49] TOCSY,[50] NOESY,[51] ROESY[52]). The chemical shift deviation for each residue of the experimental peptide ($\Delta\delta$Hα(exp)) and the folded reference peptide ($\Delta\delta$Hα(F)) was derived using eqs 1 and 2,[55] where δHα(exp) is the chemical shift from the residue of interest of the experimental peptide, δHα(U) is the chemical shift for the corresponding residue on the unfolded reference peptide, and δHα(F) is the chemical shift from the residue of interest on the folded reference peptide.

$$\Delta\delta\mathrm{H}\alpha(\mathrm{exp}) = \Delta\mathrm{H}\alpha(\mathrm{exp}) - \delta\mathrm{H}\alpha(\mathrm{U}) \quad (1)$$

$$\Delta\delta\mathrm{H}\alpha(\mathrm{F}) = \delta\mathrm{H}\alpha(\mathrm{F}) - \delta\mathrm{H}\alpha(\mathrm{U}) \quad (2)$$

Interproton Distances from NOE Cross Peaks. The NOE cross peaks for all peptides were assigned from the corresponding ROESY spectra. The intensity of each NOE cross peak was measured by the integration based on the Gaussian peak model. The distance between the two β hydrogen atoms on the proline side chain (regardless of stereochemistry) was set as the standard (1.77 Å) to derive the interproton distance for the cross peak of interest using eq 3.[56] The distances (R_{residue}) were grouped into short (≤2.5 Å), medium (2.5−3.5 Å), and long (>3.5 Å) for depiction in the Wüthrich diagrams.

$$R_{\mathrm{residue}} = 1.77 \times 10^{-10} \times \left(\frac{I_{\mathrm{standard}}}{I_{\mathrm{residue}}}\right)^{1/6} \quad (3)$$

Fraction Folded and Free Energy Folding (ΔG_{fold}). The fraction folded and free energy of folding (ΔG_{fold}) for each residue was derived from Hα chemical shift values assuming a two-state folding model for the β-hairpin peptides.[31,57] The

dx.doi.org/10.1021/bi400911p | *Biochemistry* 2013, 52, 7785−7797

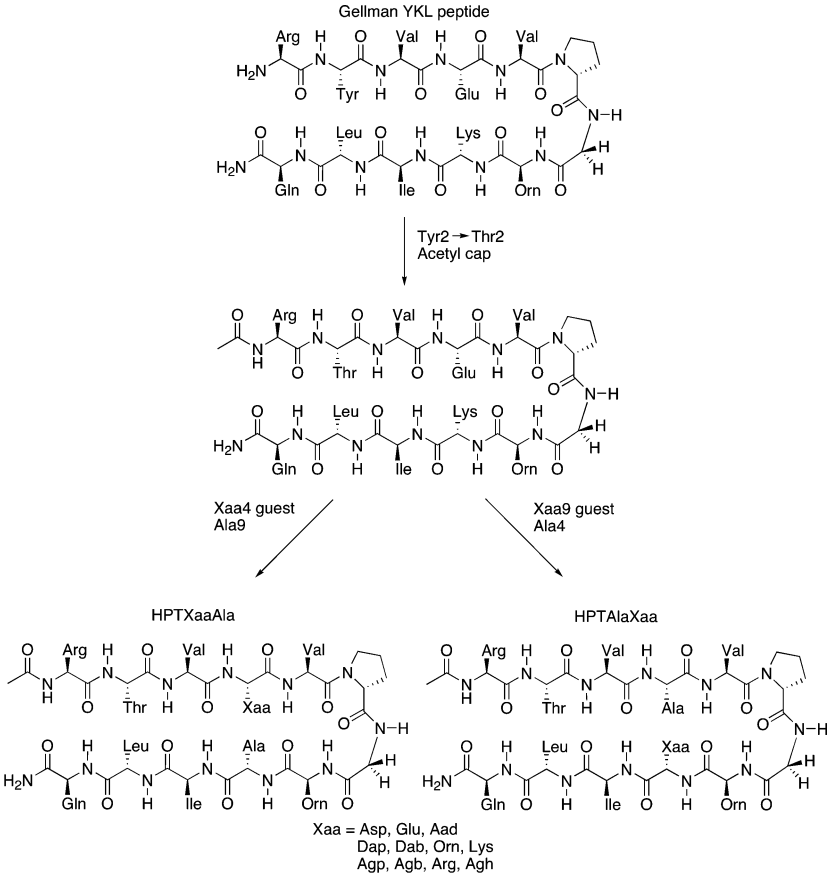

Figure 2. Design of peptides HPTXaaAla and HPTAlaXaa.

fraction folded for a given residue was derived using eq 4,[31,57] where δHα(exp) was the Hα chemical shift of the residue of interest on the experimental peptide, δHα(U) was the Hα chemical shift of the corresponding residue on the unfolded reference peptide, and δHα(F) was the Hα chemical shift of the corresponding residue on the folded reference peptide. The free energy of folding (ΔG_{fold}) for each residue was derived using eq 5.[31,57] The fraction folded and ΔG_{fold} of each peptide were determined by averaging the corresponding values for residues 2, 3, 9, and 10. For comparing the free energy of folding or fraction folded, the values were considered to be different if the Z value was greater than 0.8 (which gives a P value of 0.4 or less for the two-tailed test).

$$\text{fraction folded} = \frac{\delta\text{H}\alpha(\text{exp}) - \delta\text{H}\alpha(\text{U})}{\delta\text{H}\alpha(\text{F}) - \delta\text{H}\alpha(\text{U})} \times 100\% \quad (4)$$

$$\Delta G_{fold} = -RT \ln \frac{\delta\text{H}\alpha(\text{F}) - \delta\text{H}\alpha(\text{exp})}{\delta\text{H}\alpha(\text{exp}) - \delta\text{H}\alpha(\text{U})} \quad (5)$$

$^3J_{NH\alpha}$ Spin−Spin Coupling. The peak-to-peak separation in the absorptive (ν_a) and dispersive (ν_d) DQF-COSY spectra was measured to derive the coupling constant based on the values along the $f2$ axis unless there was significant spectral overlap. These two values were used to derive the $^3J_{NH\alpha}$ coupling constant from the square root of the single real root using eq 6.[58]

$$J^6 - {\nu_d}^2 J^4 + \left(-\frac{9}{4}{\nu_a}^4 + \frac{3}{2}{\nu_a}^2{\nu_d}^2 + \frac{3}{4}{\nu_d}^4\right)J^2 + \frac{81}{64}{\nu_a}^6 - \frac{9}{16}{\nu_a}^4{\nu_d}^2 - \frac{21}{32}{\nu_a}^2{\nu_d}^4 - \frac{1}{16}{\nu_d}^6 + \frac{{\nu_d}^8}{64{\nu_a}^2} = 0 \quad (6)$$

Survey of β-Sheet Residues in Natural Proteins. The survey was performed on PDBselect (April 2009, 25% threshold),[59,60] a database of nonredundant protein chains. The β-strand conformation and the antiparallel/parallel orientations were defined based on DSSP.[61,62] The residues on an internal and edge strand were defined based on the presence of complementary strands on both sides and on only one side using DSSP,[61,62] respectively. The non-hydrogen bonded and hydrogen bonded residues were defined based on the hydrogen bond definition using DSSP.[61,62] The corresponding sheet residues of interest were selected and the occurrences were compiled using in-house code written in ActivePerl 5.8.8.819. The statistical propensity of a given amino acid type for a given β-sheet structural context was derived by dividing the occurrence of the given amino acid type in the given β-sheet structural context by the expected occurrence based on all structures in the database. The expected occurrence and the corresponding standard deviation were obtained by bootstrapping[63] the β-sheet structural context against the entire PDBselect database. The bootstrapping was performed by running in-house code written in C++ using the high-performance computing facilities in the Computer and Information Networking Center at National Taiwan University.

dx.doi.org/10.1021/bi400911p | Biochemistry 2013, 52, 7785−7797

Table 1. Sequences for the Experimental Peptides HPTXaaAla, the Folded Reference Peptides HPTFXaaAla, and the Unfolded Reference Peptides HPTUXaaAla

peptide	sequence[a]
HPTXaaAla	Ac-Arg Thr Val Xaa Val ^{D}Pro Gly Orn Ala Ile Leu Gln-NH_2
HPTFXaaAla	Ac-Cys Arg Thr Val Xaa Val ^{D}Pro Gly Orn Ala Ile Leu Gln Cys-NH_2
HPTUXaaAla	Ac-Arg Thr Val Xaa Val Pro Gly Orn Ala Ile Leu Gln-NH_2

[a]Xaa: Asp, Glu, Aad, Dap, Dab, Orn, Lys, Agp, Agb, Arg, and Agh. A total of 33 peptides are represented in this table.

Table 2. Sequences for the Experimental Peptides HPTAlaXaa, the Folded Reference Peptides HPTFAlaXaa, and the Unfolded Reference Peptides HPTUAlaXaa

peptide	sequence[a]
HPTAlaXaa	Ac-Arg Thr Val Ala Val ^{D}Pro Gly Orn Xaa Ile Leu Gln-NH_2
HPTFAlaXaa	Ac-Cys Arg Thr Val Ala Val ^{D}Pro Gly Orn Xaa Ile Leu Gln Cys-NH_2
HPTUAlaXaa	Ac-Arg Thr Val Ala Val Pro Gly Orn Xaa Ile Leu Gln-NH_2

[a]Xaa: Asp, Glu, Aad, Dap, Dab, Orn, Lys, Agp, Agb, Arg, and Agh. A total of 33 peptides are represented in this table.

Dividing the difference between the occurrence and the expected occurrence by the standard deviation gave the Z value, which was used to obtain the P value based on a normal distribution.[64,65] The P values were obtained using the program R 2.15.2 (64-bit) on a MacBookPro (2.3 GHz Intel Core I5) running MacOSX10.7.5.

RESULTS

Peptide Design and Synthesis. The peptides were designed based on a water-soluble monomeric β-hairpin peptide YKL as described by Gellman (Figure 2).[31,66] The parent YKL β-hairpin peptide was 68% folded,[31] suitable for capturing small variations in folding percentage and energetics to investigate the effect of charged side chain length on strand stability. The positively charged amino acids Arg1, Orn8, and Lys9 were incorporated to ensure water solubility and prevent aggregation.[31] Residue Orn8 was incorporated to provide amino acid diversity and avoid NMR signal overlap, enabling facile NMR data analysis.[31] Residue ^{D}Pro6 was incorporated to promote hairpin formation.[31,67−69] In this study, the parent YKL peptide residue Tyr2 was replaced with Thr to remove the diagonal Lys9-Tyr2 cation−π interaction and to simultaneously maintain the hairpin structure (Figure 2). The N-terminus was capped with an acetyl group and the C-terminus was capped with a carboxyamide to avoid unexpected and potentially interfering electrostatic interactions involving the backbone (Figure 2).[37] The guest sites were the non-hydrogen bonding positions 4 and 9 near the center of the β-strands to avoid end fraying near the termini and excessive folding near the turn (Figure 2). Charged amino acids with varying side chain lengths were incorporated at position 4, and Ala was incorporated at position 9 to give the HPTXaaAla peptides (Table 1 and Figure 2); the peptides are named with the "HPT" prefix, representing ***H***air***P***ins with ***T***hr at position 2, followed by the three letter codes for the residues at positions 4 and 9. Incorporating Gly at position 9 would be more ideal compared to Ala to minimize lateral cross-strand interactions between residues 4 and 9. However, incorporating Gly at a strand position has been shown to give a very unstable sheet-containing protein,[23] leading to the incorporation of the slightly larger Ala instead to give a protein with reasonable stability. As such, Ala was incorporated at position 9 to provide reasonable hairpin stability and minimize (but not completely eliminate) cross-strand interactions with position 4. The charged amino acids at the guest position included negatively charged residues with a carboxylate group, positively charged residues with an ammonium group, and positively charged residues with a guanidinium group. The negatively charged residue was systematically lengthened from Asp (one methylene) to Glu (two methylenes) to (*S*)-2-aminoadipic acid (Aad, three methylenes) (Figure 1). The ammonium bearing positively charged residue was systematically shortened from Lys (4 methylenes) to Orn (3 methylenes) to (*S*)-2,4-diaminobutyric acid (Dab, 2 methylenes), and to (*S*)-2,3-diaminopropionic acid (Dap, 1 methylene) (Figure 1). The guanidinium bearing positively charged residue was systematically shortened from (*S*)-2-amino-6-guanidinohexanoic acid (Agh, 4 methylenes) to Arg (3 methylenes), to (*S*)-2-amino-4-guanidinobutyric acid (Agb, 2 methylenes), and to (*S*)-2-amino-3-guanidinopropionic acid (Agp, 1 methylene) (Figure 1). Similarly, charged amino acids with varying side chain lengths were incorporated at position 9, and Ala was incorporated at position 4 to give the HPTAlaXaa peptides (Table 2 and Figure 2). Again, this would minimize lateral cross-strand interactions between the guest position 9 residue and Ala4 due to the small side chain of Ala. However, the charged residues incorporated at position 9 in the HPTAlaXaa peptides could potentially interact with Thr2 in a diagonal fashion,[31,33] leading to results perhaps requiring both intrinsic sheet propensity and diagonal cross-strand interaction for complete interpretation. Similarly, the charged residues incorporated at position 4 in the HPTXaaAla peptides could potentially interact with Gly7 in a diagonal fashion, which should be minimal due to the inherent small size of Gly. As such, the results from the HPTXaaAla should be more straightforward to understand, requiring only intrinsic sheet propensity for interpretation. To determine the percent folded for these peptides, the fully folded and fully unfolded reference peptides would be necessary.[31−33,57] Cysteines were introduced at both the N- and C-terminus for cyclization via disulfide bond formation to give the folded reference peptides HPTFXaaAla and HPTFAlaXaa (Tables 1 and 2),[31−33,57] which are presumed to be fully folded. The turn sequence was changed from ^{D}Pro-Gly to ^{L}Pro-Gly, which should form a type II turn and disfavor hairpin formation,[31,57] to give the unfolded reference peptides HPTUXaaAla and HPTUAlaXaa (Tables 1 and 2), which are presumed to be fully unfolded. The ***f***olded and ***u***nfolded reference peptides are named by adding the letters "F" and "U" after "HPT", respectively.

The peptides were synthesized by solid phase peptide synthesis using Fmoc-based chemistry.[45,46] Peptides containing Agb were synthesized by solid phase guanidinylation following published procedures.[9,47] All peptides were purified by reverse-phase high-performance liquid chromatography to greater than 95% purity and confirmed by MALDI-TOF. No significant changes (in chemical shift or line widths) were observed in the 1D NMR spectra for peptides HPTAlaAad and HPTAlaAsp between 10 mM and 20 μM (Figures S1−S4 in the Supporting Information), suggesting that these peptides do not aggregate in this concentration range. Furthermore, peptides with positively charged residues at the guest position would bear three positive charges and should be less prone to aggregation compared to peptides with negatively charged residues at the guest position (such as HTPAlaAad and HPTAlaAsp), due to potential intermolecular electrostatic repulsion. Also, analogous peptides do not aggregate in solution.[29,31,70] As such, the peptides in this study most likely do not aggregate in solution, and the experimental data should reflect the intramolecular interactions with minimal interference from intermolecular interactions.

Nuclear Magnetic Resonance Spectroscopy and β-Hairpin Structure Characterization. The peptides were analyzed by two-dimensional NMR spectroscopy including DQF-COSY,[49] TOCSY,[50] NOESY,[51] and ROESY.[52] Sequence specific assignments for all peptides were completed by using the aforementioned 2D-NMR spectra (Tables S1−S66 in the Supporting Information).[71] The number of major spin systems correlated with the number of residues for all peptides. For HPTXaaAla, HPTAlaXaa, HPTUXaaAla, and HPTUAlaXaa peptides, extra spin systems with very weak signals were observed for Val and Gly residues in the TOCSY spectra. For the HPTAlaAgp, HPTAlaAgb, HPTAlaArg, and HPTAlaAgh peptides, other weak spin systems were also observed (Tables S19−S22 in the Supporting Information). Importantly, the number of residues for all peptides corresponded to the number of major spin systems assigned based on the major NMR signals. Chemical shift dispersion correlates to the folded population;[72] the higher the chemical shift dispersion, the higher the folded population.[72] For a given amino acid at the guest position, among the experimental HPTXaaAla peptide, the unfolded reference HPTUXaaAla peptide, and folded reference HPTFXaaAla peptide, the folded reference HPTFXaaAla peptide showed the highest dispersive chemical shifts, whereas the unfolded reference HPTUXaaAla peptide showed the least dispersive chemical shifts (Figure 3 and Tables S1−S11, S23−S33, S45−S55 in the Supporting Information). The chemical shift dispersion of the HPTXaaAla peptide was between the corresponding unfolded reference HPTUXaaAla peptide and the folded reference HPTFXaaAla peptide (Figure 3 and Tables S1−S11, S23−S33, S45−S55 in the Supporting Information). As such, the relative chemical shift dispersion was consistent with the intended relative folding for the peptides. Similar chemical shift dispersion trends were observed for the HPTAlaXaa, HPTFAlaXaa, and HPTUAlaXaa peptides (Tables S12−S22, S34−S44, S56−S66 in the Supporting Information).

Chemical shift deviation of the Hα signals ($\Delta\delta$Hα), cross-strand NOEs, and $^3J_{NH\alpha}$ spin−spin coupling constants were used to confirm hairpin formation for the folded reference peptides and the experimental HPTXaaAla and HPTAlaXaa peptides. Chemical shift deviation of Hα ($\Delta\delta$Hα) is defined as the difference between the observed chemical shift and the random coil value for the α proton.[73] A positive $\Delta\delta$Hα value is indicative of β-sheet conformation,[73] whereas a negative value is indicative of α-helical conformation.[73] In this study, the unfolded reference peptides HPTUXaaAla and HPTUAlaXaa were assumed to be random coil. The $\Delta\delta$Hα for the HPTXaaAla, HPTAlaXaa, HPTFXaaAla, and HPTFAlaXaa peptides were derived from the corresponding chemical shift values. For these peptides, a positive $\Delta\delta$Hα was observed for residues Arg1 through Val5 and residues Orn8 through Gln12,

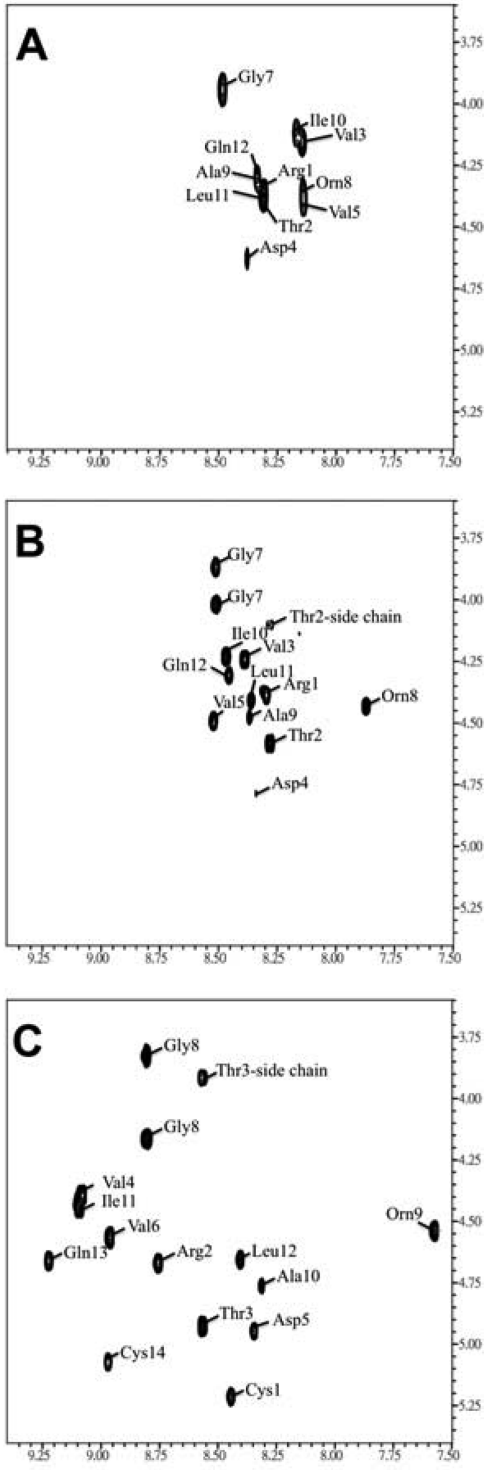

Figure 3. Chemical shift dispersion of peptides HPTUAspAla (panel A), HPTAspAla (panel B), and HPTFAspAla (panel C) based on the HCα-HN region of the TOCSY spectra.

dx.doi.org/10.1021/bi400911p | *Biochemistry* 2013, 52, 7785−7797

consistent with the formation of two β-strands (Figure 4 and Figures S5−S8 in the Supporting Information). Furthermore,

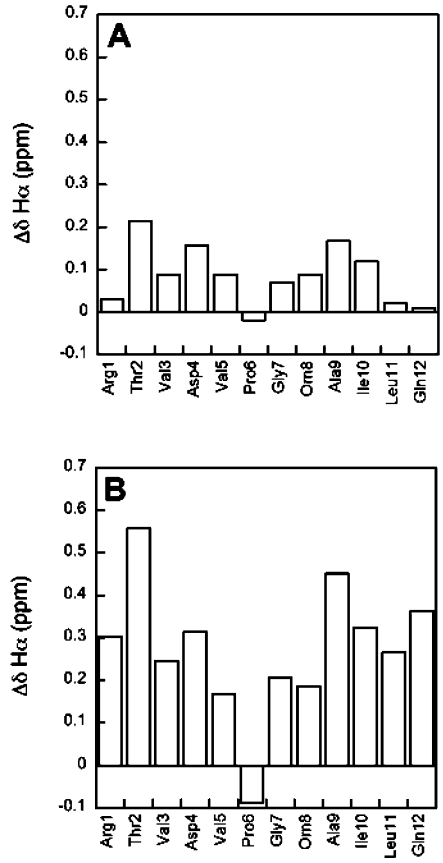

Figure 4. Chemical shift deviation ($\Delta\delta$Hα) for each residue in peptides HPTAspAla (panel A) and HPTFAspAla (panel B).

the $\Delta\delta$Hα values were higher for the inward pointing amino acid residues at the non-hydrogen bonded positions 2, 4, and 9 compared to the outward pointing residues at hydrogen bonded positions 3, 5, 8, and 10 (Figure 4 and Figures S5−S8 in the Supporting Information). This may be due to higher hydrophobicity at the inward pointing non-hydrogen bonded positions compared to the outward pointing hydrogen bonded positions.[74] Also, the $\Delta\delta$Hα was higher for Thr2 compared to Leu11, most likely due to the right-handed twist of the β-hairpin construct[31,56,57,70] and perhaps the difference in capping (acetyl versus carboxyamide) for the two termini. The $\Delta\delta$Hα values were close to zero for the residues at positions 7 and 8, consistent with turn conformation.[70]

All cross peaks in the ROESY spectra were assigned for all peptides. Sequential $d_{\alpha NH}(i, i+1)$ NOE connectivities between backbone protons were observed for the intended β-strands for all peptides (Figures S9−S96 in the Supporting Information). In contrast, the number of cross-strand NOE connectivities between backbone protons varied considerably, following the trends HPTUXaaAla < HPTXaaAla < HPTFXaaAla and HPTUAlaXaa < HPTAlaXaa < HPTFAlaXaa for a given Xaa residue at the guest position (Figures S9−S96 in the Supporting Information). The number of cross-strand NOE connectivities involving side chain protons followed the same trends (Figures S9−S74 in the Supporting Information). Since a higher number of cross-strand NOE connectivities should represent a higher folding percentage for the intended β-hairpin structure, the observed trends are consistent with the intended designs. Interestingly, most of the cross-strand NOE connectivities involving side chains were diagonal (not lateral) (Figures S9−S74 in the Supporting Information), consistent with the typical right-handed twist for β-hairpin structures.[31,56,57,70]

The $^3J_{NH\alpha}$ spin−spin coupling constant for each residue in all peptides was derived from the DQF-COSY spectra (Tables S67−S72 in the Supporting Information).[58] The $^3J_{NH\alpha}$ value of a given residue is related to the backbone dihedral ϕ, which is related to the secondary structure.[75] The $^3J_{NH\alpha}$ value for a residue in an α-helical conformation would be lower than 6 Hz,[75] whereas the $^3J_{NH\alpha}$ value for a residue in a β-sheet conformation would be higher than 7 Hz.[75] The $^3J_{NH\alpha}$ of most strand residues were higher than 7 Hz in the folded reference HPTFXaaAla and HPTFAlaXaa peptides, suggesting a β-sheet conformation for these residues (Tables S67 and S70 in the Supporting Information). Similar results were obtained for the HPTXaaAla and HPTAlaXaa peptides except for a few outliers (Tables S68 and S71 in the Supporting Information). Unfortunately, the $^3J_{NH\alpha}$ values could not be completely determined for the unfolded reference peptides HPTUXaaAla and HPTUAlaXaa due to signal overlap (Tables S69 and S72 in the Supporting Information).

Fraction Folded and ΔG_{fold}. The fraction folded for each residue of the experimental peptides was derived from the Hα chemical shifts (Figure 5 and Figures S97 and S98 in the

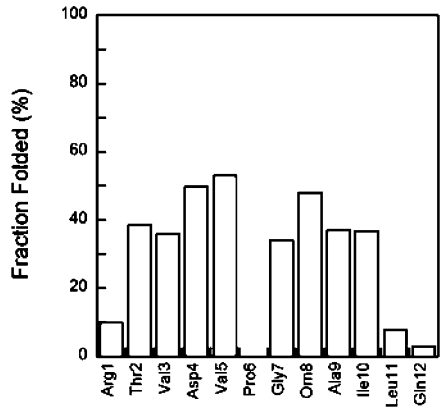

Figure 5. Fraction folded of each residue in peptide HPTAspAla.

Supporting Information).[31,57] The unfolded reference peptides HPTUXaaAla and HPTUAlaXaa with Pro6 were assumed to represent the fully unfolded form of the experimental peptides HPTXaaAla and HPTAlaXaa, respectively.[31,57] Also, the disulfide cyclized folded reference peptides HPTFXaaAla and HPTFAlaXaa were assumed to represent the fully folded form of the experimental peptides HPTXaaAla and HPTAlaXaa, respectively.[31−33,57] The ratio of the chemical shift deviation ($\Delta\delta$Hα) for a given residue of the experimental peptide (HPTXaaAla or HPTAlaXaa) and the chemical shift deviation of the corresponding residue of the folded reference peptide (HPTFXaaAla and HPTFAlaXaa) gave the fraction folded for the residue of interest in the experimental peptide (Figure 5 and Figures S97 and S98 in the Supporting Information).[23,42] The fraction folded of Arg1 and Gln12 for the HPTXaaAla and HPTAlaXaa peptides was relatively lower than the other residues due to end fraying effects (Figure 5 and Figures S97 and S98 in the Supporting Information). Furthermore, the

dx.doi.org/10.1021/bi400911p | *Biochemistry* 2013, 52, 7785−7797

fraction folded for the residues increased with increasing distance from the N- and C-termini, reaching a maximum value at residues Val5 and Orn8, respectively. These results are consistent with a well-folded β-hairpin conformation promoted by the turn. For the HPTXaaAla and the HPTAlaXaa peptides, the fraction folded of the residues on the N-terminal strand was higher compared to the fraction folded of the corresponding residues on the C-terminal strand with the same distance from the corresponding termini, perhaps due to the right-handed twist. For example, the fraction folded for Leu11 was consistently lower than the fraction folded for Thr2. Focusing on the non-hydrogen bonded inward pointing residues, the fraction folded for positions 4 and 9 were consistently higher than the percent folded for positions 2 and 11, most likely due to end fraying effects.

The fraction folded for a given peptide was represented by the average of the fraction folded for residues at positions 2, 3, 9, and 10 (Figures 6 and 7 and Tables 3 and 4).[23,42] These residues were selected to provide equal representation for the hydrogen bonded (3 and 10) and non-hydrogen bonded positions (2 and 9), avoid artifacts due to turn-promoted sheet conformation and end fraying effects, and account for unequal folding of the two strands. The fraction folded ranged from 19% to 40% for the HPTXaaAla peptides (Figure 6 and Table 3), whereas the values ranged from 14% to 30% for the HPTAlaXaa peptides (Figure 7 and Table 4). The standard deviation for the fraction folded for the peptides was 1−5%. However, the standard deviation for the fraction folded for the HPTXaaAla peptides was somewhat smaller than the standard deviation for the fraction folded for the HPTAlaXaa peptides (Figures 6 and 7 and Tables 3 and 4). The fraction folded of the HPTXaaAla peptides with Lys analogues at the guest position followed the trend: HPTDapAla < HPTDabAla < HPTOrnAla ~ HPTLysAla (Figure 6A). Similarly, the fraction folded of the HPTAlaXaa peptides with Lys analogues at the guest position followed the trend: HPTAlaDap ~ HPTAlaDab < HPTAlaOrn ~ HPTAlaLys (Figure 7A). The fraction folded of the HPTXaaAla peptides with Arg analogues at the guest position followed the trend: HPTAgbAla < HPTArgAla < HPTAghAla < HPTAgpAla (Figure 6B). Similarly, the fraction folded of the HPTAlaXaa peptides with Arg analogues at the guest position followed the trend: HPTAlaAgb < HPTAlaArg ~ HPTAlaAgp < HPTAlaAgh (Figure 7B). As such, the fraction folded seemed to roughly increase with increasing side chain length of the positively charged residue at the guest position for peptides HPTXaaAla and HPTAlaXaa (Figures 6 and 7). The exceptionally high fraction folded for the Agp-containing peptides (Figures 6B and 7B) may be due to the close proximity of the bulky guanidinium group to the backbone for Agp, because larger side chains can favor the sheet conformation by destabilizing alternative structures through steric interactions.[76,77] The fraction folded of HPTXaaAla peptides with Asp analogues at the guest position followed the trend: HPTAspAla > HPTGluAla > HPTAadAla (Figure 6C), whereas the fraction folded of HPTAlaXaa peptides with Asp analogues at the guest position followed the opposite trend: HPTAlaAsp < HPTAlaGlu < HPTAlaAad (Figure 7C). These two trends for the negatively charged residues appear to contradict one another, most likely because the two guest positions are nonequivalent (see Discussion).

The folding free energy (ΔG_{fold}) for each peptide was derived from the chemical shift data from residues 2, 3, 9, and 10 assuming a two-state folding process for the peptides

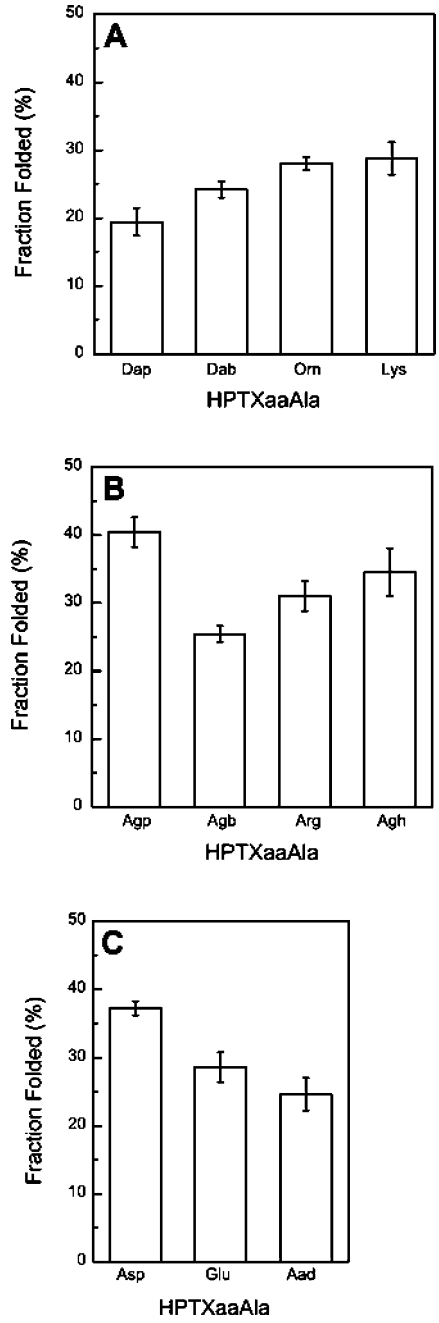

Figure 6. Fraction folded for the HPTXaaAla peptides (Xaa = Dap, Dab, Orn, Lys, Agp, Agb, Arg, Agh, Asp, Glu, Aad).

(Tables 3 and 4).[31,57] The more positive the ΔG_{fold}, the less stable the peptide β-hairpin structure. Compared to the parent YKL peptide (H-Arg-Tyr-Val-DPro-Gly-Orn-Lys-Ile-Leu-Gln-NH_2),[31] peptide HPTAlaLys was 1 kcal/mol less stable due to the simultaneous loss of the cross-strand diagonal Lys-Tyr cation−π interation and lateral Glu-Lys ion pairing interaction. Compared to the analogous VKL peptide (Ac-Arg-Val-Val-Glu-Asn-Gly-Orn-Lys-Ile-Leu-Gln-NH_2),[44] peptide HPTAlaLys was 0.4 kcal/mol less stable due to the loss of the cross-strand lateral Glu-Lys ion pairing interaction. The ΔG_{fold} for HPTXaaAla peptides with Lys analogues at the guest position followed the trend: HPTLysAla ~ HPTOrnAla < HPTDabAla < HPTDapAla (Table 3). For these four peptides, the stability increased with increasing side chain length from one to three

dx.doi.org/10.1021/bi400911p | Biochemistry 2013, 52, 7785−7797

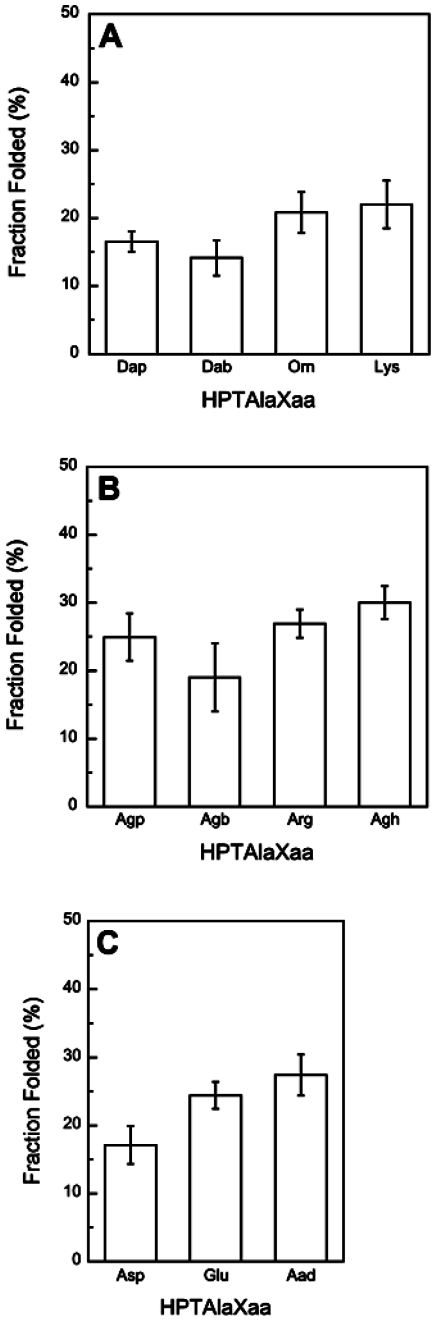

Figure 7. Fraction folded for the HPTAlaXaa peptides (Xaa = Dap, Dab, Orn, Lys, Agp, Agb, Arg, Agh, Asp, Glu, Aad).

methylenes (Dap, Dab, and Orn); however, adding another methylene to Orn (to give Lys) did not increase the peptide stability further. Similarly, the ΔG_{fold} for HPTAlaXaa peptides with Lys analogues at the guest position followed the trend: HPTAlaLys ~ HPTAlaOrn < HPTAlaDab ~ HPTAlaDap (Table 4). These four peptides apparently could be separated into two groups based on stability. The peptides with shorter side chains (one and two methylenes for Dap and Dab) were less stable compared to peptides with longer side chains (three and four methylenes for Orn and Lys). In general, the ΔG_{fold} appeared to decrease with increasing side chain length of the Lys analogue, regardless of the non-hydrogen bonded guest position. The difference in ΔG_{fold} for Lys- and Dab-containing peptides was smaller in our guest systems (HPTAlaXaa and HPTXaaAla) compared to the VKL system,[44] most likely due to the lack of cross-strand lateral Glu-Lys/Dab ion pairing interactions. Apparently, the overall stability of the hairpin system affects the energy difference upon altering the Lys side chain length.

Table 3. Fraction Folded (%)[a] and ΔG_{fold} (kcal/mol)[b] of HPTXaaAla Peptides

peptide	fraction folded (%)[a]	ΔG_{fold} (kcal/mol)[b]
HPTAspAla	37 ± 1	0.31 ± 0.02
HPTGluAla	29 ± 2	0.54 ± 0.07
HPTAadAla	25 ± 2	0.67 ± 0.08
HPTDapAla	19 ± 2	0.85 ± 0.07
HPTDabAla	24 ± 1	0.68 ± 0.04
HPTOrnAla	28 ± 1	0.56 ± 0.03
HPTLysAla	29 ± 2	0.54 ± 0.07
HPTAgpAla	40 ± 3	0.23 ± 0.06
HPTAgbAla	25 ± 1	0.64 ± 0.04
HPTArgAla	31 ± 2	0.47 ± 0.06
HPTAghAla	34 ± 3	0.38 ± 0.09

[a]Average of fraction folded for residues 2, 3, 9, and 10. [b]Average of ΔG_{fold} for residues 2, 3, 9, and 10.

Table 4. Fraction Folded (%)[a] and ΔG_{fold} (kcal/mol)[b] of HPTAlaXaa Peptides

peptide	fraction folded (%)[a]	ΔG_{fold} (kcal/mol)[b]
HPTAlaAsp	17 ± 3	0.93 ± 0.12
HPTAlaGlu	24 ± 2	0.67 ± 0.06
HPTAlaAad	27 ± 3	0.58 ± 0.09
HPTAlaDap	16 ± 1[c]	0.96 ± 0.06[c]
HPTAlaDab	14 ± 3	1.1 ± 0.1
HPTAlaOrn	21 ± 3	0.80 ± 0.11
HPTAlaLys	22 ± 3	0.75 ± 0.12
HPTAlaAgp	25 ± 4	0.66 ± 0.12
HPTAlaAgb	19 ± 5	0.88 ± 0.21
HPTAlaArg	27 ± 2	0.59 ± 0.06
HPTAlaAgh	30 ± 2	0.50 ± 0.07

[a]Average of fraction folded for residues 2, 3, 9, and 10. [b]Average of ΔG_{fold} for residues 2, 3, 9, and 10. [c]Average of values for residues 2, 3, and 10.

The ΔG_{fold} for HPTXaaAla peptides with Arg analogues at the guest position followed the trend: HPTAgpAla < HPTAghAla < HPTArgAla < HPTAgbAla (Table 3). Similarly, the ΔG_{fold} for HPTAlaXaa peptides with Arg analogues at the guest position followed the trend: HPTAlaAgh < HPTAlaArg ~ HPTAlaAgp < HPTAlaAgb (Table 4). Accordingly, the ΔG_{fold} appeared to decrease with increasing side chain length of the Arg analogue except for Agp, which exhibited exceptionally low ΔG_{fold} upon incorporation most likely caused by conformation restrictions due to sterics.[76,77] The overall change in ΔG_{fold} upon altering the guanidinium bearing side chain length was similar to the ΔG_{fold} change upon altering the ammonium bearing side chain length. The ΔG_{fold} for HPTXaaAla peptides with Asp analogues at the guest position followed the trend: HPTAspAla < HPTGluAla < HPTAadAla (Table 3), whereas the ΔG_{fold} HPTAlaXaa peptides with Asp analogues at the guest position followed the opposite trend: HPTAlaAsp > HPTAlaGlu > HPTAlaAsp (Table 4). These two trends strongly suggest that the two non-hydrogen bonded strand positions 4 and 9 are nonequivalent (see Discussion),

dx.doi.org/10.1021/bi400911p | Biochemistry 2013, 52, 7785−7797

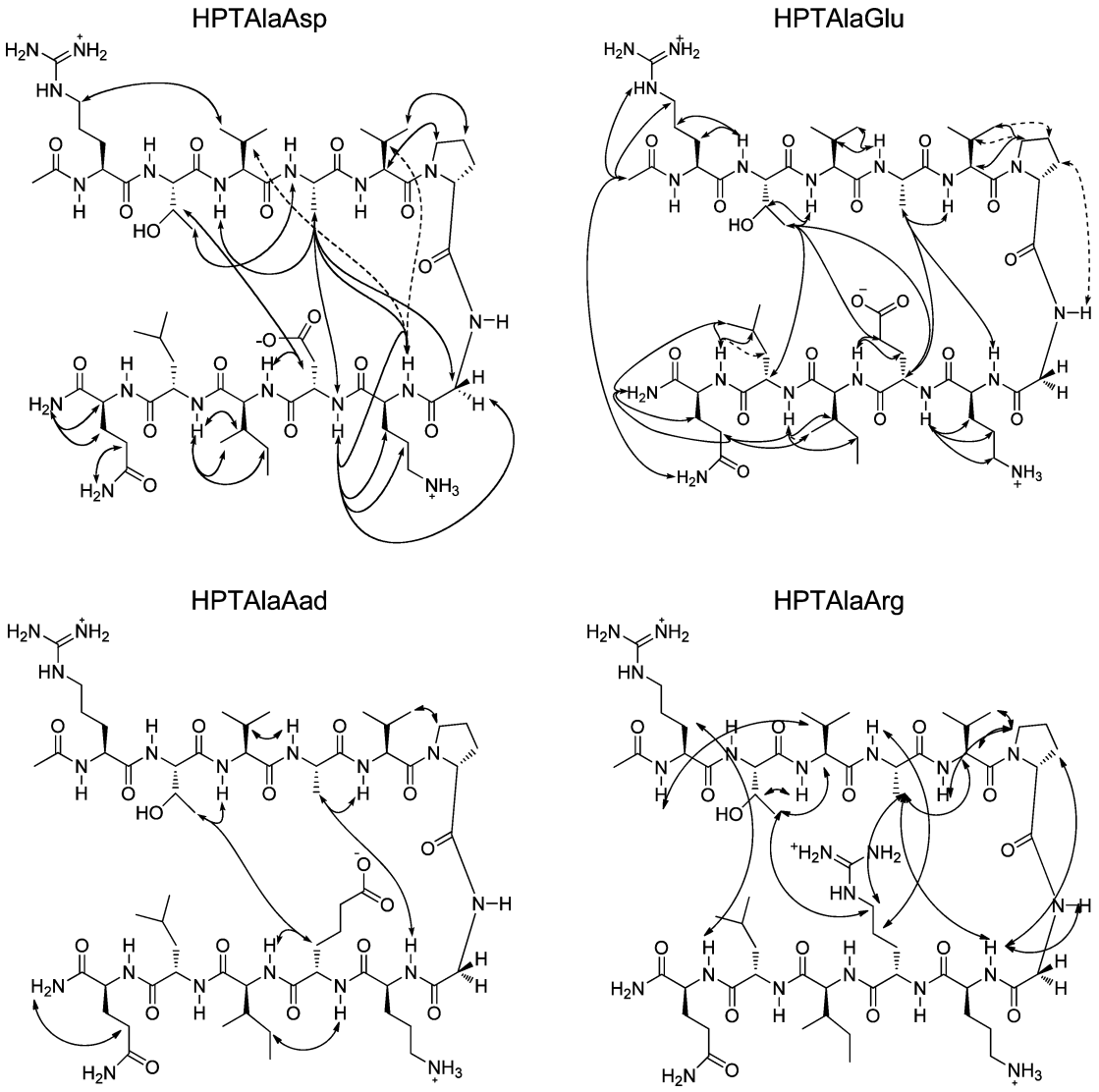

Figure 8. The inter-residue NOEs involving side chain protons for peptides HPTAlaAsp, HPTAlaGlu, HPTAlaAad, and HPTAlaArg.

even though similar trends were observed for the positively charged residues with varying side chain length.

DISCUSSION

The effect of varying the side chain length on charged amino acids at non-hydrogen bonded strand positions in a β-hairpin was explored by NMR methods. Both positively charged and negatively charged amino acids were investigated at a non-hydrogen bonded position on the N-terminal strand (HPTXaaAla peptides) and C-terminal strand (HPTAlaXaa peptides). For peptides containing Lys analogues with varying side chain length (Lys, Orn, Dab, Dap), the fraction folded decreased and the ΔG_{fold} increased with decreasing side chain length (Figures 6 and 7 and Tables 3 and 4), consistent with the trends obtained using an analogous hairpin construct.[44] The stability for peptides with the guest position on the N-terminal strand followed the trend HPTAgpAla > HPTAghAla > HPTArgAla > HPTAgbAla (Table 3). In this series, the fraction folded decreased and the ΔG_{fold} increased with decreasing side chain length except for the Agp-containing peptide. Similarly, the stability for peptides with the guest position on the C-terminal strand followed the trend HPTAlaAgh > HPTAlaArg ~ HPTAlaAgp > HPTAlaAgb (Table 4). In both of these series, the Agp-containing peptides exhibited exceptionally high fraction folded and low ΔG_{fold}, most likely because the short Agp side chain brings the bulky guanidinium group close to the backbone to limit the backbone conformations to sheet-like structures through steric interactions with the backbone.[76,77] Nonetheless, the fraction folded and ΔG_{fold} of the Agb-containing peptides exhibited the lowest fraction folded and the highest ΔG_{fold} (Figures 6B and 7B and Tables 3 and 4). Interestingly, the RNA binding specificity and cellular uptake of Tat (human immunodeficiency virus type 1, transactivation of transcription protein)-derived peptides increased upon shortening the Arg side chain length by one methylene to Agb,[47] perhaps suggesting the importance of low sheet stability of Agb for both activities.

The stability trends were opposite one another for the peptides incorporating the negatively charged Asp analogues (Asp, Glu, Aad) at the two different non-hydrogen bonded guest positions 4 and 9 (Figures 6C and 7C and Tables 3 and 4). The hairpin stability decreased with increasing side chain length for peptides with the negatively charged residue at the N-terminal strand guest position 4. This trend is the opposite of the trend observed for the peptides incorporating Lys

dx.doi.org/10.1021/bi400911p | *Biochemistry* 2013, 52, 7785−7797

analogues (regardless of the guest position). In contrast, the hairpin stability increased with increasing side chain length for peptides with the negatively charged residue at the C-terminal strand guest position 9. This trend is the same as the trend for the peptides containing Lys analogues at the guest position (regardless of the guest position).

The guest site at position 4 for the HPTXaaAla peptides is an inward pointing non-hydrogen bonded position on the N-terminal strand. For residues with a given positively charged functionality at the guest position, the hairpin stability of the HPTXaaAla peptides increased with increasing side chain length (except for Agp) (Table 3), consistent with increasing sheet propensity with increasing side chain size and hydrophobicity.[76−80] Surprisingly, for the negatively charged residues at guest position 4, the hairpin stability for HPTXaaAla decreased with increasing side chain length (Table 3), apparently contradicting current understanding of sheet propensity. Although the guest position 4 of HPTXaaAla can potentially interact with Gly7 through cross-strand diagonal hydrophobic interactions, this interaction would be very weak due to the inherent small size of Gly. The guest position 4 could also interact with Ala9 through cross-strand lateral hydrophobic interactions, which should increase with increasing side chain length. However, the branched bulky carboxylate functionality can limit the backbone conformations to sheet-like structures through steric interactions with the backbone[76,77] as the side chain length becomes shorter. This shape-based steric argument is consistent with the repeatedly observed high thermodynamic sheet propensity for the β-branched amino acids,[20−23] and could also explain the exceptionally high stability for both Agp-containing peptides (HPTAgpAla and HPTAlaAgp). Since the overall side chain length and branching shape of Agp is similar to Glu, the steric effect on conformation should be present for Glu and be even more pronounced for Asp, leading to the increased stability with decreasing side chain length for the negatively charged residues at position 4.

The guest site at position 9 for the HPTAlaXaa peptides is an inward pointing non-hydrogen bonded position on the C-terminal strand. For a given side chain functionality, the hairpin stability for HPTAlaXaa roughly increased with increasing side chain length, consistent with increasing sheet propensity with increasing side chain size and hydrophobicity.[76−80] However, diagonal cross-strand interactions between positions 2 and 9 were observed in the parent YKL β-hairpin due to the right-handed twist.[28,31] In the HPTAlaXaa peptides, diagonal cross-strand NOE connectivities between Thr2 and Xaa9 were also observed for HPTAlaAsp, HPTAlaGlu, HPTAlaAad, and HPTAlaArg (Figures 8 and 9). Furthermore, Xaa9 may interact with Ala4 through lateral cross-strand hydrophobic interactions, with NOE connnectivities between the two side chains for some of the peptides (Figures S9−S74 in the Supporting Information). These potential cross-strand hydrophobic interactions should increase with increasing side chain length to stabilize the hairpin structure. The observed stability trends for HPTAlaXaa peptides are consistent with the cross-strand diagonal interaction with Thr2 and cross-strand lateral interaction with Ala4, completely overriding the steric effects of the negatively charged residues and partially offsetting the steric effects of Agp.

The sheet forming energetics for the natural charged amino acids (Asp, Glu, Lys, Arg) determined based on the protein G B1 domain exhibited context dependence,[21−23] similar to the work reported here. The stability of the zinc-finger host peptide

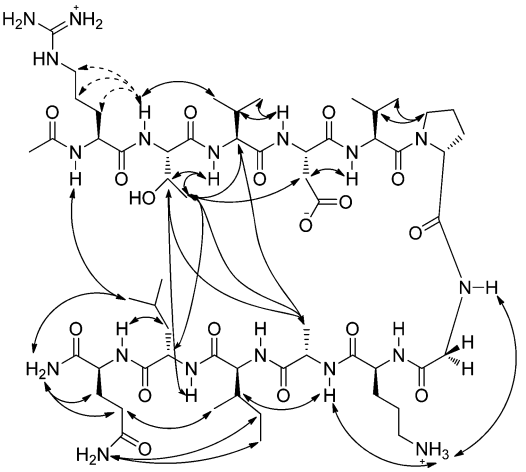

Figure 9. Inter-residue NOEs involving side chain protons for peptide HPTAspAla.

with charged amino acids incorporated on a β-strand followed the trends Asp ∼ Glu and Arg > Lys based on metal ion binding assays.[20] The similar stability for Asp and Glu is different from our results, whereas the Arg > Lys stability trend is consistent with our results from HPTAlaXaa peptides but not those from HPTXaaAla peptides. Although the zinc finger host system[20] is more similar to our antiparallel β-hairpin compared to the protein G B1 domain,[21−23] differences in stability trends remain, again suggesting differences in detailed context for the systems.

The thermodynamic effects of incorporating charged amino acids at sheet positions in proteins provided varying trends. To provide further insight into the incorporation of charged amino acids at non-hydrogen bonding positions of antiparallel edge strands in sheet structures of natural proteins, the non-redundant protein structure database PDBselect (April 2009, 25% threshold)[59,60] was surveyed. Out of the 666 086 residues in the database, 150 934 adopted a sheet conformation as defined by DSSP,[61,62] amounting to around 23%. The statistical sheet propensity for the charged residues followed the trends Glu > Asp and Arg > Lys (Table S73 in the Supporting Information). These same trends were observed when only edge strands were analyzed (Table S74 in the Supporting Information), limiting the survey to edge strands in antiparallel β-sheets (Table S75 in the Supporting Information) or even further limiting the survey to only non-hydrogen bonded positions on edge strands in antiparallel sheets (Table S76 in the Supporting Information). Interestingly, the statistical propensity trends are consistent with our stability trends for the HPTAlaXaa peptides but not those for the HPTXaaAla peptides. Importantly, the statistical propensity trends for incorporating the charged residues into sheet structures appeared to remain constant regardless of structural context (edge versus internal, antiparallel versus parallel, hydrogen bonded versus non-hydrogen bonded), even though these trends may not match all of the experimentally determined thermodynamic trends.

■ CONCLUSIONS

The effect of varying the charged amino acid side chain length in a β-hairpin has been studied for two non-hydrogen bonded guest positions. The hairpin stability mostly increased with increasing side chain length for positively charged Lys and Arg

dx.doi.org/10.1021/bi400911p | Biochemistry 2013, 52, 7785−7797

analogues except for Agp, which provided exceptionally high hairpin stability most likely due to sterics near the backbone. In contrast, hairpin peptides with negatively charged Asp analogues showed length dependence with opposite trends depending on guest position due to the nonequivalence of the two guest positions. Importantly, these results should facilitate the use of charged amino acids with varying side chain lengths to modulate sheet structure stability and to develop β-hairpin based materials.[81−85]

■ ASSOCIATED CONTENT

Supporting Information

Materials and methods section with details of the synthesis and characterization of the peptides, chemical shift assignment data, chemical shift deviation data, coupling constant data, diagrams indicating NOE connnectivities, and survey results. This material is available free of charge via the Internet at http://pubs.acs.org.

■ AUTHOR INFORMATION

Corresponding Author

*Phone: +886-2-33669789. Fax: +886-2-33668671. E-mail: rpcheng@ntu.edu.tw.

Funding

This work was supported by National Taiwan University (R.P.C.) and the National Science Council in Taiwan (L.H.K., NSC-99-2815-C-002-076-M; J.H.L., NSC-100-2815-C-002-001-M; S.J.H., NSC-100-2731-M-002-002-MY2; R.P.C., NSC-98-2119-M-002-025, NSC-99-2113-M-002-002-MY2, NSC-101-2113-M-002-006-MY2).

Notes

The authors declare no competing financial interest.

■ ACKNOWLEDGMENTS

The authors would like to thank the Computer and Information Networking Center at National Taiwan University for the support of the high-performance computing facilities.

■ ABBREVIATIONS

Aad, (*S*)-aminoadipate; Agb, (*S*)-2-Amino-4-guanidinobutyric acid; Agh, (*S*)-2-Amino-6-guanidinohexanoic acid; Agp, (*S*)-2-Amino-3-guanidinopropionic acid; Ala, alanine; Arg, arginine; Asp, aspartate; Dab, (*S*)-2,4-diaminobutyric acid; Dap, (*S*)-2,3-diaminopropionic acid; DQF-COSY, double-quantum filtered-correlated spectroscopy; Fmoc, *N*-9-fluorenylmethyloxycarbonyl; Glu, glutamate; Lys, lysine; MALDI-TOF, matrix-assisted laser desorption ionization time-of-flight; NMR, nuclear magnetic resonance spectroscopy; NOESY, nuclear Overhauser effect spectroscopy; Orn, ornithine; ROESY, rotating-frame nuclear Overhauser effect spectroscopy; TOCSY, total correlation spectroscopy

■ REFERENCES

(1) Creighton, T. E. (1993) *Proteins: Structure and Molecular Properties*, 2nd ed., W. H. Freeman and Co., New York.

(2) Fersht, A. R. (1999) *Structure and Mechanism in Protein Science. A Guide to Enzyme Catalysis and Protein Folding*, W. H. Freeman and Co., New York.

(3) Baldwin, R. L., and Rose, G. D. (1999) Is protein folding hierarchic? I. Local structure and peptide folding. *Trends Biochem. Sci. 24*, 26−33.

(4) Baldwin, R. L., and Rose, G. D. (1999) Is protein folding hierarchic? II. Folding intermediates and transition states. *Trends Biochem. Sci. 24*, 77−83.

(5) Chou, P. Y., and Fasman, G. D. (1974) Conformational parameters for amino acids in helical, β-sheet, and random coil regions calculated from proteins. *Biochemistry 13*, 211−222.

(6) Engel, D. E., and DeGrado, W. F. (2004) Amino acid propensities are position-dependent throughout the length of α-helices. *J. Mol. Biol. 337*, 1195−1205.

(7) Cheng, R. P., Girinath, P., Suzuki, Y., Kuo, H.-T., Hsu, H.-C., Wang, W.-R., Yang, P.-A., Gullickson, D., Wu, C.-H., Koyack, M. J., Chiu, H.-P., Weng, Y.-J., Hart, P., Kokona, B., Fairman, R., Lin, T.-E., and Barrett, O. (2010) Positional effects on helical Ala-based peptides. *Biochemistry 49*, 9372−9384.

(8) Cheng, R. P., Wang, W.-R., Girinath, P., Yang, P.-A., Ahmad, R., Li, J.-H., Hart, P., Kokona, B., Fairman, R., Kilpatrick, C., and Argiros, A. (2012) Effect of glutamate side chain length on intrahelical glutamate-lysine ion pairing interactions. *Biochemistry 51*, 7157−7172.

(9) Cheng, R. P., Weng, Y.-J., Wang, W.-R., Koyack, M. J., Suzuki, Y., Wu, C.-H., Yang, P.-A., Hsu, H.-C., Kuo, H.-T., Girinath, P., and Fang, C.-J. (2012) Helix formation and capping energetics of arginine analogs with varying side chain length. *Amino Acids 43*, 195−206.

(10) Donald, J. E., Kulp, D. W., and DeGrado, W. F. (2011) Salt bridges: Geometrically specific, designable interactions. *Proteins 79*, 898−915.

(11) Munoz, V., and Serrano, L. (1994) Intrinsic secondary structure propensities of the amino acids, using statistical φ-ψ matrices: Comparison with experimental scales. *Proteins 20*, 301−311.

(12) Palmer, M. S., Dryden, A. J., Hughes, J. T., and Collinge, J. (1991) Homozygous prion protein genotype predisposes to sporadic Creutzfeldt-Jakob disease. *Nature 352*, 340−342.

(13) Johnson, R. T., and Gibbs, C. J., Jr. (1998) Creutzfeldt-Jakob disease and related transmissible spongiform encephalopathies. *N. Engl. J. Med. 339*, 1994−2004.

(14) Beal, M. F., Kowall, N. W., Ellison, D. W., Mazurek, M. F., Swartz, K. J., and Martin, J. B. (1986) Replication of the neurochemical characteristics of Huntington's disease by quinolinic acid. *Nature 321*, 168−171.

(15) Walker, F. O. (2007) Huntington's disease. *Lancet 369*, 218−228.

(16) Luo, Y., Bolon, B., Kahn, S., Bennett, B. D., Babu-Khan, S., Denis, P., Fan, W., Kha, H., Zhang, J. H., Gong, Y. H., Martin, L., Louis, J. C., Yan, Q., Richards, W. G., Citron, M., and Vassar, R. (2001) Mice deficient in BACE1, the Alzheimer's β-secretase, have normal phenotype and abolished β-amyloid generation. *Nat. Neurosci. 4*, 231−232.

(17) Citron, M. (2010) Alzheimer's disease: Strategies for disease modification. *Nat. Rev. Drug Discovery 9*, 387−398.

(18) Feany, M. B., and Bender, W. W. (2000) A Drosophila model of Parkinson's disease. *Nature 404*, 394−398.

(19) Dauer, W., and Przedborski, S. (2003) Parkinson's disease: Mechanisms and models. *Neuron 39*, 889−909.

(20) Kim, C. W. A., and Berg, J. M. (1993) Thermodynamic β-sheet propensities measured using a zinc-finger host peptide. *Nature 362*, 267−270.

(21) Minor, D. L., and Kim, P. S. (1994) Measurement of the β-sheet-forming propensities of amino acids. *Nature 367*, 660−663.

(22) Minor, D. L., and Kim, P. S. (1994) Context Is a major determinant of β-sheet propensity. *Nature 371*, 264−267.

(23) Smith, C. K., Withka, J. M., and Regan, L. (1994) A thermodynamic scale for the β-sheet forming tendencies of the amino acids. *Biochemistry 33*, 5510−5517.

(24) Smith, C. K., and Regan, L. (1995) Guidelines for protein design: The energetics of β sheet side chain interactions. *Science 270*, 980−982.

(25) Merkel, J. S., and Regan, L. (1998) Aromatic rescue of glycine in β sheets. *Fold. Des. 3*, 449−455.

(26) Merkel, J. S., Sturtevant, J. M., and Regan, L. (1999) Sidechain interactions in parallel β sheets: The energetics of cross-strand pairings. *Structure 7*, 1333−1343.
(27) Blasie, C. A., and Berg, J. M. (1997) Electrostatic interactions across a β-sheet. *Biochemistry 36*, 6218−6222.
(28) Russell, S. J., and Cochran, A. G. (2000) Designing stable β-hairpins: Energetic contributions from cross-strand residues. *J. Am. Chem. Soc. 122*, 12600−12601.
(29) Russell, S. J., Blandl, T., Skelton, N. J., and Cochran, A. G. (2003) Stability of cyclic β-hairpins: Asymmetric contributions from side chains of a hydrogen-bonded cross-strand residue pair. *J. Am. Chem. Soc. 125*, 388−395.
(30) Ramirez-Alvarado, M., Blanco, F. J., and Serrano, L. (2001) Elongation of the BH8 β-hairpin peptide: Electrostatic interactions in β-hairpin formation and stability. *Protein Sci. 10*, 1381−1392.
(31) Syud, F. A., Stanger, H. E., and Gellman, S. H. (2001) Interstrand side chain-side chain interactions in a designed β-hairpin: Significance of both lateral and diagonal pairings. *J. Am. Chem. Soc. 123*, 8667−8677.
(32) Tatko, C. D., and Waters, M. L. (2002) Selective aromatic interactions in β-hairpin peptides. *J. Am. Chem. Soc. 124*, 9372−9373.
(33) Tatko, C. D., and Waters, M. L. (2003) The geometry and efficacy of cation-π interactions in a diagonal position of a designed β-hairpin. *Protein Sci. 12*, 2443−2452.
(34) Laughrey, Z. R., Kiehna, S. E., Riemen, A. J., and Waters, M. L. (2008) Carbohydrate-π interactions: What are they worth? *J. Am. Chem. Soc. 130*, 14625−14633.
(35) Riemen, A. J., and Waters, M. L. (2010) Dueling post-translational modifications trigger folding and unfolding of a β-hairpin peptide. *J. Am. Chem. Soc. 132*, 9007−9013.
(36) Wouters, M. A., and Curmi, P. M. G. (1995) An analysis of side chain interactions and pair correlations within antiparallel β-sheets: The differences between backbone hydrogen-bonded and non-hydrogen-bonded residue pairs. *Proteins 22*, 119−131.
(37) Searle, M. S., Griffiths-Jones, S. R., and Skinner-Smith, H. (1999) Energetics of weak interactions in a β-hairpin peptide: Electrostatic and hydrophobic contributions to stability from lysine salt bridges. *J. Am. Chem. Soc. 121*, 11615−11620.
(38) Kiehna, S. E., and Waters, M. L. (2003) Sequence dependence of β-hairpin structure: Comparison of a salt bridge and an aromatic interaction. *Protein Sci. 12*, 2657−2667.
(39) Ciani, B., Jourdan, M., and Searle, M. S. (2003) Stabilization of β-hairpin peptides by salt bridges: Role of preorganization in the energetic contribution of weak interactions. *J. Am. Chem. Soc. 125*, 9038−9047.
(40) Chakrabartty, A., Kortemme, T., and Baldwin, R. L. (1994) Helix propensities of the amino-acids measured in alanine-based peptides without helix-stabilizing side-chain interactions. *Protein Sci. 3*, 843−852.
(41) Padmanabhan, S., York, E. J., Stewart, J. M., and Baldwin, R. L. (1996) Helix propensities of basic amino acids increase with the length of the side-chain. *J. Mol. Biol. 257*, 726−734.
(42) Doig, A. J., and Baldwin, R. L. (1995) N- and C-capping preferences for all 20 amino acids in α-helical peptides. *Protein Sci. 4*, 1325−1336.
(43) Sueki, M., Lee, S., Powers, S. P., Denton, J. B., Konishi, Y., and Scheraga, H. A. (1984) Helix coil stability constants for the naturally occurring amino acids in Water. 22. Histidine parameters from random poly[(hydroxybutyl)glutamine-*co*-L-histidine]. *Macromolecules 17*, 148−155.
(44) Hughes, R. M., Benshoff, M. L., and Waters, M. L. (2007) Effects of chain length and N-methylation on a cation-π interaction in a β-hairpin peptide. *Chem.—Eur. J. 13*, 5753−5764.
(45) Atherton, E., Fox, H., Harkiss, D., Logan, C. J., Sheppard, R. C., and Williams, B. J. (1978) A mild procedure for solid phase peptide synthesis: Use of fluorenylmethoxycarbonylamino-acids. *J. Chem. Soc. Chem. Comm.*, 537−539.
(46) Fields, G. B., and Noble, R. L. (1990) Solid phase peptide synthesis utilizing 9-fluorenylmethoxycarbonyl amino acids. *Int. J. Pept. Protein Res. 35*, 161−214.
(47) Wu, C.-H., Chen, Y.-P., Mou, C.-Y., and Cheng, R. P. (2013) Altering the Tat-derived peptide bioactivity landscape by changing the arginine side chain length. *Amino Acids 44*, 473−480.
(48) Volkmer-Engert, R., Landgraf, C., and Schneider-Mergener, J. (1998) Charcoal surface-assisted catalysis of intramolecular disulfide bond formation in peptides. *J. Pept. Res. 51*, 365−369.
(49) Aue, W. P., Bartholdi, E., and Ernst, R. R. (1976) Two-dimensional spectroscopy. Application to nuclear magnetic resonance. *J. Chem. Phys. 64*, 2229−2246.
(50) Bax, A., and Davis, D. G. (1985) MLEV-17-based two-dimensional homonuclear magnetization transfer spectroscopy. *J. Magn. Reson. 65*, 355−360.
(51) Jeener, J., Meier, B. H., Bachmann, P., and Ernst, R. R. (1979) Investigation of exchange processes by two-dimensional NMR spectroscopy. *J. Chem. Phys. 71*, 4546−4553.
(52) Bothner-By, A. A., Stephens, R. L., Lee, J.-m., Warren, C. D., and Jeanloz, R. W. (1984) Structure determination of a tetrasaccharide: Transient nuclear Overhauser effects in the rotating frame. *J. Am. Chem. Soc. 106*, 811−813.
(53) Piotto, M., Saudek, V., and Sklenar, V. (1992) Gradient-tailored excitation for single-quantum NMR spectroscopy of aqueous solutions. *J. Biomol. NMR 2*, 661−665.
(54) Sklenar, V., Piotto, M., Leppik, R., and Saudek, V. (1993) Gradient-tailored water suppression for 1H-15N HSQC experiments optimized to retain full sensitivity. *J. Magn. Reson., Ser A 102*, 241−245.
(55) Wishart, D. S., Sykes, B. D., and Richards, F. M. (1991) Relationship between nuclear magnetic resonance chemical shift and protein secondary structure. *J. Mol. Biol. 222*, 311−333.
(56) Ramirez-Alvarado, M., Kortemme, T., Blanco, F. J., and Serrano, L. (1999) β-Hairpin and β-sheet formation in designed linear peptides. *Bioorg. Med. Chem. 7*, 93−103.
(57) Syud, F. A., Espinosa, J. F., and Gellman, S. H. (1999) NMR-based quantification of β-sheet populations in aqueous solution through use of reference peptides for the folded and unfolded states. *J. Am. Chem. Soc. 121*, 11577−11578.
(58) Kim, Y. M., and Prestegard, J. H. (1989) Measurement of vicinal couplings from cross peaks in COSY spectra. *J. Magn. Reson. 84*, 9−13.
(59) Hobohm, U., and Sander, C. (1994) Enlarged representative set of protein structures. *Protein Sci. 3*, 522−524.
(60) Griep, S., and Hobohm, U. (2010) PDBselect 1992−2009 and PDBfilter-select. *Nucleic Acids Res. 38*, D318−D319.
(61) Kabsch, W., and Sander, C. (1983) Dictionary of protein secondary structure: Pattern recognition of hydrogen-bonded and geometrical features. *Biopolymers 22*, 2577−2637.
(62) Joosten, R. P., Beek, T. A. H. T., Krieger, E., Hekkelman, M. L., Hooft, R. W. W., Schneider, R., Sander, C., and Vriend, G. (2011) A series of PDB related databases for everyday needs. *Nucleic Acids Res. 39*, D411−D419.
(63) Efron, B., and Gong, G. (1983) A leisurely look at the bootstrap, the jackknife, and cross-validation. *Amer. Stat. 37*, 36−48.
(64) Klugh, H. E. (1970) *Statistics: the essentials for research*, p 350, John Wiley & Sons, Inc., New York.
(65) Kuebler, R. R., and Smith, H. (1976) *Statistics-A beginning*, p 302, John Wiley & Sons, Inc., New York.
(66) Stanger, H. E., and Gellman, S. H. (1998) Rules for antiparallel β-sheet design: D-Pro-Gly is superior to L-Asn-Gly for β-hairpin nucleation. *J. Am. Chem. Soc. 120*, 4236−4237.
(67) Struthers, M. D., Cheng, R. P., and Imperiali, B. (1996) Economy in protein design: Evolution of a metal-independent ββα motif based on the zinc finger domains. *J. Am. Chem. Soc. 118*, 3073−3081.
(68) Cheng, R. P., Fisher, S. L., and Imperiali, B. (1996) Metallopeptide design: Tuning the metal cation affinities with unnatural amino acids and peptide secondary structure. *J. Am. Chem. Soc. 118*, 11349−11356.

(69) Struthers, M. D., Cheng, R. P., and Imperiali, B. (1996) Design of a monomeric 23-residue polypeptide with defined tertiary structure. *Science 271*, 342−345.
(70) Ramirez-Alvarado, M., Blanco, F. J., and Serrano, L. (1996) De novo design and structural analysis of a model β-hairpin peptide system. *Nat. Struct. Biol. 3*, 604−612.
(71) Wüthrich, K. (1986) *NMR of Proteins and Nucleic Acids*, John Wiley & Sons, New York.
(72) Yao, J., Dyson, H. J., and Wright, P. E. (1997) Chemical shift dispersion and secondary structure prediction in unfolded and partly folded proteins. *FEBS Lett. 419*, 285−289.
(73) Dalgarno, D. C., Levine, B. A., and Williams, R. J. P. (1983) Structural information from NMR secondary chemical shifts of peptide α C-H protons in proteins. *Biosci. Rep. 3*, 443−452.
(74) Maynard, A. J., Sharman, G. J., and Searle, M. S. (1998) Origin of β-hairpin stability in solution: Structural and thermodynamic analysis of the folding of a model peptide supports hydrophobic stabilization in water. *J. Am. Chem. Soc. 120*, 1996−2007.
(75) Pardi, A., Billeter, M., and Wüthrich, K. (1984) Calibration of the angular dependence of the amide proton-C^{α} proton coupling constants, $^{3}J_{HN\alpha}$, in a Globular Protein. Use of $^{3}J_{HN\alpha}$ for identification of helical secondary structure. *J. Mol. Biol. 180*, 741−751.
(76) Bai, Y., and Englander, S. W. (1994) Hydrogen bond strength and β-sheet propensities: The role of a side chain blocking effect. *Proteins 18*, 262−266.
(77) Street, A. G., and Mayo, S. L. (1999) Intrinsic β-sheet propensities result from van der Waals interactions between side chains and the local backbone. *Proc. Natl. Acad. Sci. U.S.A. 96*, 9074−9076.
(78) Yang, A.-S., and Honig, B. (1995) Free energy determinants of secondary structure formation: II. Antiparallel β-sheets. *J. Mol. Biol. 252*, 366−376.
(79) Otzen, D. E., and Fersht, A. R. (1995) Side-chain determinants of β-sheet stability. *Biochemistry 34*, 5718−5724.
(80) Koehl, P., and Levitt, M. (1999) Structure-based conformational preferences of amino acids. *Proc. Natl. Acad. Sci. U.S.A. 96*, 12524−12529.
(81) Schneider, J. P., Pochan, D. J., Ozbas, B., Rajagopal, K., Pakstis, L., and Kretsinger, J. (2002) Responsive hydrogels from the intramolecular folding and self-assembly of a designed peptide. *J. Am. Chem. Soc. 124*, 15030−15037.
(82) Haines, L. A., Rajagopal, K., Ozbas, B., Salick, D. A., Pochan, D. J., and Schneider, J. P. (2005) Light-activated hydrogel formation via the triggered folding and self-assembly of a designed peptide. *J. Am. Chem. Soc. 127*, 17025−17029.
(83) Salick, D. A., Kretsinger, J. K., Pochan, D. J., and Schneider, J. P. (2007) Inherent antibacterial activity of a peptide-based β-hairpin hydrogel. *J. Am. Chem. Soc. 129*, 14793−14799.
(84) Nagarkar, R. P., Hule, R. A., Pochan, D. J., and Schneider, J. P. (2008) De novo design of strand-swapped β-hairpin hydrogels. *J. Am. Chem. Soc. 130*, 4466−4474.
(85) Nagy, K. J., Giano, M. C., Jin, A., Pochan, D. J., and Schneider, J. P. (2011) Enhanced mechanical rigidity of hydrogels formed from enantiomeric peptide assemblies. *J. Am. Chem. Soc. 133*, 14975−14977.